

Identifying a sphenoid sinus fungus ball using a nomogram model*

Yu-Hsi Fan^{1,†}, Pei-Wen Wu^{2,3,†}, Yen-Lin Huang⁴, Cheng-Chi Lee^{3,5},
Ta-Jen Lee^{2,3,6}, Chi-Che Huang^{2,7}, Po-Hung Chang^{2,7}, Chien-Chia Huang^{2,3,7}

Rhinology 61: 2, 153 - 160, 2023

<https://doi.org/10.4193/Rhin22.329>

¹ Department of Medical Education, Chang Gung Memorial Hospital and Chang Gung University, Taoyuan, Taiwan

² Division of Rhinology, Department of Otolaryngology, Chang Gung Memorial Hospital and Chang Gung University, Taoyuan, Taiwan

³ School of Medicine, Chang Gung University, Taoyuan, Taiwan

⁴ Department of Anatomic Pathology, Chang Gung Memorial Hospital and Chang Gung University, Taoyuan, Taiwan

⁵ Department of Neurosurgery, Chang Gung Memorial Hospital at Linkou and Chang Gung University, Taiwan.

⁶ Department of Otolaryngology, Xiamen Chang Gung Hospital, Xiamen, China

⁷ Graduate Institute of Clinical Medical Sciences, College of Medicine, Chang Gung University, Taiwan

***Received for publication:**

August 20, 2022

Accepted: November 11, 2022

[†] contributed equally to this work

Abstract

Background: Sphenoid sinus fungus ball (SSFB) is a rare entity and usually presents with non-specific symptoms. SSFB could potentially lead to serious orbital and intracranial complications. Computed tomography (CT) scan is usually the first imaging test of the diagnostic workup in patients with specific clinical symptoms. This study aimed to compare the clinical characteristics and CT features between SSFB and unilateral (non-fungus ball) chronic sphenoid rhinosinusitis (USRS) and help differentiate between these two most common inflammatory diseases of the sphenoid sinus.

Methods: By retrospective database review, 66 patients with a histopathologic diagnosis of isolated SSFB were recruited for analysis. Fifty-four patients who underwent endoscopic sinus surgery with clinical and histopathological diagnoses of USRS were enrolled as the control group. Clinical characteristics and CT features were evaluated.

Results: Headache, rhinorrhoea, nasal obstruction, postnasal dripping, and hyposmia were the most common symptoms in both groups. In the univariate analysis, older age, lower white blood cell counts, irregular surface, bony dehiscence, lateral wall sclerosis, and intralesional hyperdensity (IH) were significant predictors for SSFB. Older age, irregular surface, and IH remained statistically significant in the multivariate analysis. Based on the results of the regression analysis, a nomogram for predicting the probability of SSFB was plotted.

Conclusions: We developed a nomogram model as a novel preoperative diagnostic tool for identifying SSFB according to the predictors both in clinical characteristics and on CT features. This could help the clinicians in predicting the probability of SSFB, to reduce ineffective or delayed treatment and occurrence of complications.

Key words: computed tomography, fungus ball, intralesional hyperdensity, sphenoid sinus, rhinosinusitis

Introduction

Fungal rhinosinusitis (FRS) is defined as a sinonasal inflammation caused by fungi, which consists of a wide range of forms of fungus related diseases, from asymptomatic to highly fatal ⁽¹⁾. FRS can be broadly classified as invasive and non-invasive forms based on the histopathologic evidence of fungus penetrating host tissue. Invasive FRS is a rare but aggressive form, particularly affecting immunocompromised patients ⁽²⁾. Non-invasive

FRS contains two different forms of extramucosal diseases, sinus fungal ball (SFB) and allergic fungal rhinosinusitis, and mostly occurs in non-immunocompromised individuals ^(3,4). However, non-invasive FRS such as SFB may progress to the invasive form when the host immunity deteriorates ⁽⁵⁾. SFB is the most common form of non-invasive FRS and is characterized by aggregation and conglomerate of fungal hyphae separate from but adjacent to the respiratory mucosa in the sinus

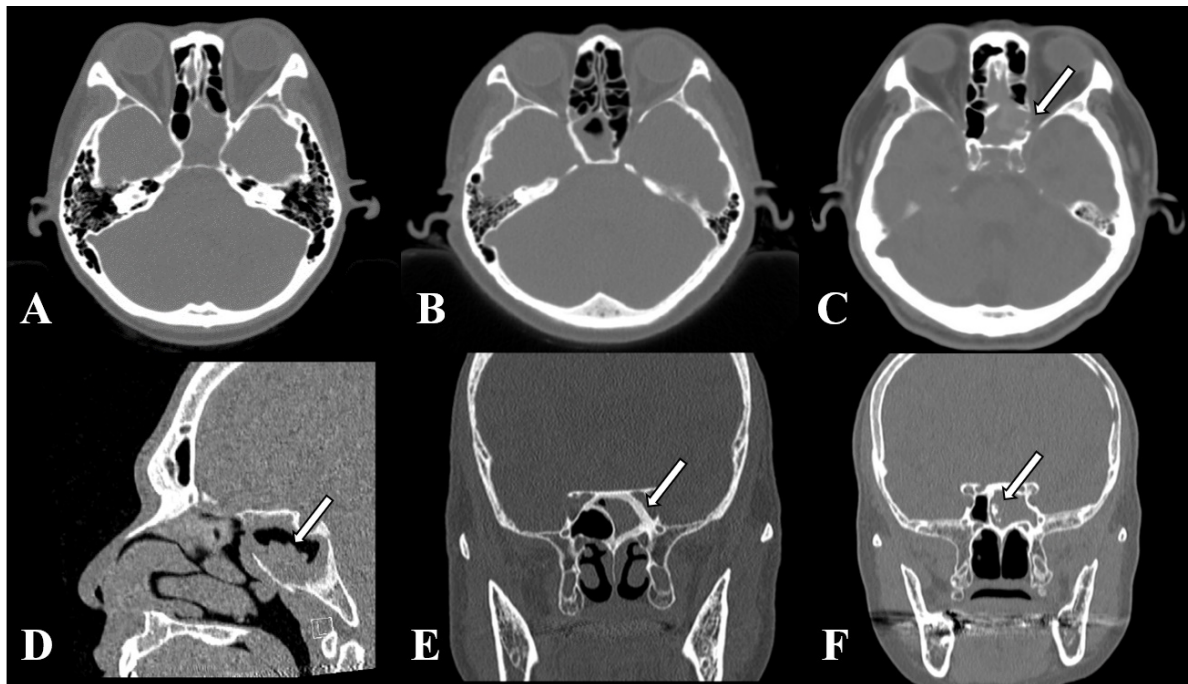


Figure 1. Computed tomographic features of sphenoid sinus lesions. (A) total opacification, (B) partial opacification, (C) bony dehiscence, (D) irregular surface, (E) lateral wall sclerosis, and (F) intralesional hyperdensity.

cavity⁽⁶⁾. SFB is mainly caused by *Aspergillus* species and involves mostly the maxillary sinus or sphenoid sinus in few patients⁽⁷⁾. Older age, female sex, diabetes mellitus, adjacent maxillary odontogenic pathology, and impaired mucosal immunity have been associated with SFB^(4,7). Medical therapy has no role in the treatment of SFB because of the significant side effects of systemic anti-fungal agents. Additionally, surgical eradication of SFB by endoscopic sinus surgery usually achieves good outcomes and has been the treatment of choice^(8,9). However, the clinical presentations of SFB are usually similar to those of other chronic rhinosinusitis^(7,10). As a result, SFB is susceptible to be overlooked or diagnosed late by clinicians in the early stage. Sphenoid sinus fungal ball (SSFB) accounts for 8% to 14.4% of SFB^(7,11) and 24% to 49% of inflammatory sphenoid sinus diseases^(12,13). Given that the sphenoid sinus is located at the depths of the skull base and abuts many vital structures, SSFB misdiagnosis or treatment delay can lead to potentially serious conditions, including orbital and intracranial complications^(14,15). This makes timely and accurate diagnosis of SSFB exceedingly important.

Radiological examination plays a vital role in the preoperative diagnosis of SFB⁽¹⁶⁾. Computed tomography (CT) has been the most frequently used imaging modality in evaluating rhinosinusitis due to its ability to depict fine images of bone, soft tissue, and blood vessels and to determine if the sinuses are obstructed⁽¹⁷⁾. Several CT imaging features of SFB have been previously reported, which includes lesion limited to a single sinus, intralesional hyperdensity (IH), bony erosion of sinus walls, bony sclerosis

of sinus walls, and irregular surface of intrasinus lesion^(16,18). IH was defined as micro-calcifications or calcification spots noted inside the sinonasal lesion, which is the most specific imaging feature of SFB, with highest specificity as 93.1% to 100%^(16,18,19). However, according to previous literature, the prevalence of IH on CT image of patients with SFB ranges from 51% to 71%, which means that the diagnosis of SFB remains challenging for a proportion of SFB patients without IH on their CT images^(3,7,16). Due to the rarity of SSFB, the diagnostic features of SSFB on CT images have not yet been widely examined. IH was reported to present on 47.2% to 69.6% of CT images in patients with SSFB and is similar to those in maxillary sinuses, the most specific diagnostic features of SSFB on CT images^(11,20,21). Besides, bony erosion and bony sclerosis of sinus walls are also commonly detected on CT images of patients with SSFB⁽²⁰⁻²²⁾. However, evaluation of the irregular surface of intrasinus lesion on CT images and the diagnostic criteria of these features for SSFB is still lacking. Therefore, the objective of this study was to investigate the clinical characteristics and the CT imaging features of SSFB and create a preoperative diagnostic algorithm for SSFB, to assist clinicians in the diagnosis and treatment decisions for patient with suspected SSFB.

Methods

Patients

We performed an automatic search of the histopathology database at Chang Gung Memorial Hospital, and 72 patients who underwent endoscopic sinus surgery with final histopatho-

Table 1. Demographic and clinical characteristics of the study populations.

Variables	SSFB (n = 66)	USRS (n = 54)	P value
Age, years (mean ± SD)	57.9 ± 14.4	47.0 ± 17.4	< 0.001***
Sex			
Male, n	18 (27.3%)	21 (38.9%)	0.177
Female, n	48 (72.7%)	33 (61.1%)	
Site of sphenoid lesion			
Left, n	28 (42.4%)	25 (46.3%)	0.356
Right, n	33 (50.0%)	28 (51.9%)	
Single sphenoid sinus, n	5 (7.6%)	1 (1.9%)	
Laboratory data			
WBC count, per µl	6623 ± 1803	7521 ± 2737	0.043*
Underlying conditions			
Diabetes mellitus, n	15 (22.7%)	2 (3.7%)	<0.001***
Malignant neoplasms, n	5 (7.6%)	4 (7.4%)	0.508
Previous sphenoid sinus surgery, n	6 (9.1%)	15 (27.8%)	0.096
Clinical presentations			
Headache and facial pain, n	31 (47.0%)	27 (50.0%)	0.744
Rhinorrhea, n	29 (43.9%)	25 (46.3%)	0.798
Purulent rhinorrhea, n	15 (22.7%)	15 (27.8%)	0.532
Bloody rhinorrhea, n	8 (12.1%)	4 (7.4%)	0.386
Nasal obstruction, n	25 (37.9%)	23 (42.6%)	0.604
Post nasal dripping, n	24 (36.4%)	21 (38.9%)	0.779
Hyposmia, n	9 (13.6%)	10 (18.5%)	0.476
Foul odor smell, n	7 (10.6%)	4 (7.4%)	0.543
Vision loss, n	5 (7.6%)	4 (7.4%)	0.521
Tinnitus, n	3 (4.5%)	0 (0%)	0.083
Incidental found, n	7 (10.6%)	2 (3.7%)	0.138

SSFB, sphenoid sinus fungus ball; USRS, unilateral sphenoid rhinosinusitis; SD, standard deviation; WBC, white blood cell. *P < 0.05, ***P < 0.001.

logic diagnosis of SSFB between 2005 and 2021 were identified. Through manual review of their preoperative CT images of the paranasal sinus and medical records, six patients with bilateral sphenoid sinuses involvement were excluded due to the difficulty in evaluating the bony sclerosis of sinus wall. The remaining 66 patients with isolated SSFB were recruited for analysis. To construct a control group, 54 patients who underwent endoscopic sinus surgery with clinical and histopathological diagnoses of unilateral chronic sphenoid rhinosinusitis (USRS, non-fungus ball) at our institute, and had no previous diagnosis of FRS were enrolled as the USRS group. All participants in the study had

received preoperative CT of the paranasal sinuses without intravenous contrast enhancement and histological examinations of the surgical specimens.

CT scans

Demographic data of patients were collected from their medical records, including their age, sex, underlying comorbidity, clinical presentations, and laboratory examination. Images of the paranasal sinus CT for each patient were carefully interpreted, and the following features of image were then documented, including the site of sphenoid lesion, total or partial opacification, irregular surface of intrasinus lesion, bony dehiscence, lateral wall sclerosis, and IH (Figure 1). Irregular surface was defined as the presence of a rough surface of the partial opacified lesion. Bony dehiscence was defined as the loss of bone in the walls of the sphenoid sinus. Lateral wall thickness was measured at the thickest point of the lateral antral wall on the coronal CT images (Figure 1E). Lateral wall sclerosis was defined as the ratio of the lateral wall of the diseased sinus to that of the contralateral sinus greater than 1.2. IH referred to the presence of focal high-density area within the intrasinus lesion.

Statistical analysis

Categorical variables are represented as frequencies and percentages, and continuous variables are represented as means ± standard deviations. To compare the variables between the SSFB and USRS groups, Chi-square test or Fisher's exact test was utilized for categorical variables, and Student's t-test or Mann-Whitney U test were employed for continuous variables. Sensitivity, specificity, positive predictive value (PPV), and negative predictive value (NPV) for each feature of the CT imaging were calculated to assess the diagnostic accuracy for SSFB. Univariate and multivariate logistic regression analyses were then used to assess the associations between SSFB and variables by calculating odds ratios with 95% confidence intervals. Based on the results of the logistic regression model, a nomogram model was plotted for predicting the probabilities of SSFB. The receiver operating characteristic (ROC) curve, the area under the ROC curve (AUC), and the calibration curve were constructed to measure the predictive performance of the nomogram model. Analyses were performed by using SPSS Statistics v26.0. (SPSS Inc., Chicago, IL, USA) and RStudio v2022.02.1 (RStudio, Boston, MA, USA). P values of less than 0.05 were regarded as statistically significant. This study was approved by the institutional review board of Chang Gung Medical Foundation (approval number: 202201253B0). The requirement for informed consent was waived in view of the retrospective nature of the research and anonymity of the data.

Results

Clinical characteristics of the study population

Table 2. Features on CT imaging of study participants.

Features	SSFB	USRS	P value	Spe	Sen	PPV	NPV
Total opacification, n	30 (45.5%)	24 (44.4%)	0.913	55.60%	45.50%	55.60%	45.50%
Partial opacification, n	36 (54.6%)	30 (55.6%)	0.913	44.40%	54.50%	54.50%	44.40%
Irregular surface, n	21 (31.8%)	6 (11.1%)	0.001**	80.00%	58.30%	77.80%	61.50%
Bony dehiscence, n	22 (33.3%)	9 (16.7%)	0.034*	83.30%	33.30%	71.00%	50.60%
Lateral wall sclerosis, n	50 (78.1%)	23 (44.2%)	< 0.001***	57.40%	75.80%	68.50%	66.00%
Intralesional hyperdensity, n	39 (59.1%)	2 (3.7%)	< 0.001***	96.30%	59.10%	95.10%	65.80%

CT, computed tomography; SSFB, sphenoid sinus fungus ball; USRS, unilateral sphenoid rhinosinusitis; Spe, specificity; Sen: sensitivity; PPV, positive predictive value; NPV, negative predictive value. *P < 0.05, **P < 0.01, ***P < 0.001.

Table 3. Logistic regression analyses of the associated factors of sphenoid sinus fungus balls.

Variables	Univariate analysis		Multivariate analysis	
	Odds Ratio (95% CI)	P value	Odds Ratio (95% CI)	P value
Characteristics				
Age	1.04 (1.02-1.07)	0.001**	1.07 (1.01-1.14)	0.027*
Diabetes mellitus	2.94 (0.99-8.71)	0.052	2.32 (0.26-20.48)	0.448
Female sex (female versus male)	1.70 (0.79-3.67)	0.178	2.87 (0.50-16.45)	0.238
WBC (x1000 per µl)	0.83 (0.70-0.99)	0.045*	0.96 (0.71-1.28)	0.757
CT imaging features				
Total opacification	1.04 (0.51-2.15)	0.912		
Partial opacification	0.96 (0.47-1.98)	0.912		
Irregular surface	5.60 (1.84-17.05)	0.002**	6.57 (1.12-38.52)	0.037*
Bony dehiscence	2.50 (1.04-6.03)	0.041*	1.15 (0.10-12.90)	0.911
Lateral wall sclerosis	4.50 (2.01-10.09)	< 0.001***	0.67 (0.13-3.51)	0.633
Intralesional hyperdensity	37.56 (8.42-167.49)	< 0.001***	42.12 (7.75-228.87)	< 0.001***

CI, confidence interval; WBC, white blood cell; CT, computed tomography. *P < 0.05, **P < 0.01, ***P < 0.001.

Characteristics of participants in the SSFB group (n = 66) and USRS group (n = 54) are summarized in Table 1. The mean age of patients in the SSFB group was significantly higher than that of the USRS group (57.9 ± 14.4 and 47.0 ± 17.4, respectively, p < 0.001). Female predominance was observed in both the groups, with women accounting for 72.7% of the SSFB group and 61.1% of the USRS group. There was a significantly higher proportion of patients with diabetes in the SSFB group than in the USRS group (22.7% and 3.7%, respectively, p < 0.001). In both the SSFB and USRS groups, the ranking of the five most prevalent symptoms was similar; namely, headache and facial pain (47.0% for SSFB and 50.0% for USRS), rhinorrhoea (43.9% and 46.3%), nasal obstruction (37.9% and 42.6%), postnasal dripping (36.4% and 38.9%), and hyposmia (13.6% and 18.5%, respectively).

Features of CT imaging

The comparisons in the features of CT imaging between the

SSFB and USRS groups are presented in Table 2. The sensitivity, specificity, positive predictive values (PPV), and negative predictive values (NPV) for each feature of the CT imaging in distinguishing SSFB were calculated therefrom. Irregular surface, bony dehiscence, lateral wall sclerosis, and IH were all significantly more common in the SSFB group than in the USRS group. Furthermore, IH, bony dehiscence, and irregular surface had the highest specificity (96.3%, 83.3%, and 80.0%, respectively) and PPV (95.1%, 71.0%, and 77.8%, respectively). Lateral wall sclerosis and intralesional hyperdensity had the highest sensitivity (75.8% and 59.1%, respectively) and NPV (66.0% and 65.8%, respectively).

Logistic regression analysis

The associations between the variables and SSFB were examined by logistic regression analysis (Table 3). In the univariate analysis, older age (OR 1.04; 95% CI 1.02-1.07), lower white blood

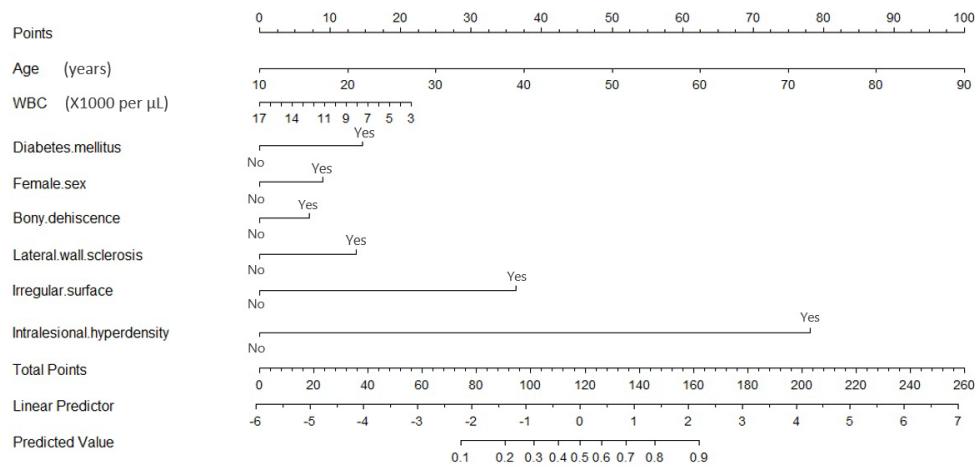


Figure 2. Nomogram for predicting sphenoid sinus fungus ball. To use this nomogram, first, find the corresponding position on each variable; second, draw a line vertically to the points axis above to get respective points, and finally, add up the points from all 7 variables and draw a line from the corresponding position on the total points axis to the predicted value axis to determine the probabilities of a fungus ball. WBC, white blood cell count.

cell (WBC) count (OR 0.83; 95% CI 0.70-1.00), irregular surface (OR 5.60; 95% CI 1.84-17.05), bony dehiscence (OR 2.50; 95% CI 1.04-6.03), lateral wall sclerosis (OR 4.50; 95% CI 2.01-10.09), and IH (OR 37.56; 95% CI 8.42-167.49) were significant predictors for SSFB (P value < 0.05). However, older age (OR 1.07; 95% CI 1.022-1.12), irregular surface (OR 5.78; 95% CI 1.81-18.58), and IH (OR 42.12; 95% CI 7.75-228.87) remained statistically significant in the multivariate analysis.

Nomogram for predicting SSFB

Based on the logistic regression model, a nomogram for predicting the probability of SSFB was plotted (Figure 2). In the nomogram, each value of a variable represents its score. By adding up the corresponding scores from all the eight variables, the total points can be obtained and the predicted value of SSFB for an individual can be derived. An example of our participant with demonstrating the use of the nomogram to predict the possibility of SSFB was showed in Supplementary Materials. The ROC curve illustrated the good discrimination ability of the nomogram with an AUC of 0.906 (95%CI 0.875-0.937) (Figure 3a). Calibration curves for the unadjusted nomogram model and the bias-corrected model were plotted overlaid on a diagonal, representing an ideal model with perfect prediction (Figure 3b). Using the calibration curves, the nomogram model slightly underestimates the probability of SSFB when the nomogram-predicted probability is between 0.25 and 0.80, and marginally overestimates the actual probability of SSFB when the predicted probability is below 0.25 or above 0.80. However, the close correspondence of the three curves represents the good calibration of the present nomogram model.

Discussion

A rapid and accurate diagnosis of SSFB is crucial in avoiding un-

necessary medical treatment and reducing the risk of potential serious complication. SSFB is a rare and insidious condition that usually presents with non-specific symptoms⁽²¹⁾. This study revealed similar clinical symptoms observed in patients with SSFB and USRS, including headache and facial pain, rhinorrhoea, nasal obstruction, postnasal dripping, and hyposmia. Therefore, clinicians should always consider the possibility of SSFB in patients with atypical headaches or chronic/recurrent rhinosinusitis after proper medical treatment. A CT scan should be performed as the first imaging test of the diagnostic workup in patients with specific clinical symptoms. If opacification in the sphenoid sinus is noted, it needs aggressive management, such as histological verification.

In this study, we further compared the features of CT imaging between patients with SSFB and USRS, and demonstrated that irregular surface, bony dehiscence, lateral wall sclerosis, and IH were all significant predictors for SSFB. Among these predictors, IH is the most specific and had an OR of 37.56 and 42.12 to associate with SSFB in the univariate and multivariate analysis, respectively. IH is related to the metal components in fungal hyphae, which further accumulate during the metabolic processes of fungi and present as hyper-attenuation on CT⁽²³⁾. In this study, IH was present in 59.1% CT images of SSFB: this was a relatively lower proportion compared to those of maxillary SFB, in which IH was present from 60-80% of cases^(4,7,16). These findings indicated that IH is a strong predictor of SSFB on CT images; however, there are still more than 40% of SSFB cases that cannot be identified by solely this feature. Thus, a comprehensive interpretation of CT images and clinical variables is necessary to achieve the most precise diagnosis.

Irregular surface, defined as the rough surface of the intrasinus lesion, was also highly associated with SSFB in the regression analyses. The presence of irregular surface represents the

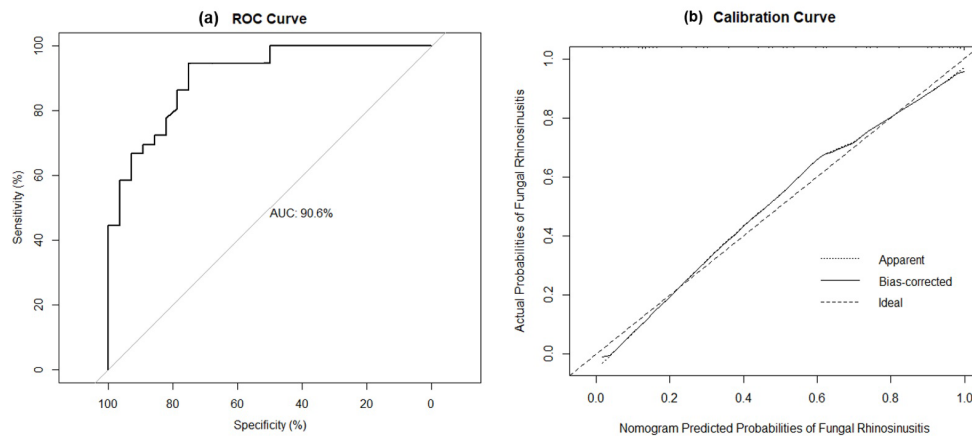


Figure 3. (a) Receiver operating characteristic (ROC) curve of the nomogram model in predicting sphenoid sinus fungus ball (SSFB). The value of the area under ROC curve (AUC) was 0.906 (95% confidence interval of 0.875–0.937). (b) Calibration curve of the nomogram model in predicting SSFB. The Ideal line represents the ideal model which predicted probabilities perfectly matching the actual probabilities. The Apparent line and the Bias-corrected line respectively represent the nomogram model before and after bootstrap re-sampling method.

intertwined mass of fungal hyphae with a coarse and irregular surface, and sometimes a sharp or serrated protrusions may be observed⁽¹⁶⁾. As for the USRS, swollen mucosa or free pus in the sinuses often appear as smooth surfaces or air-fluid levels on CT images. However, this finding can only be observed in some cases (31.8%) with partial opacification on the CT image of SSFB, depending on the amount of intrasinus mucous and fungus ball. This incidence was lower than that observed in the maxillary SFBs, in which more than 80% of cases have partial opacification exhibiting irregular surface of the intrasinus lesion^(7,16). A smaller antrum of sphenoid sinus may be the main reason for this discrepancy.

Bony remodelling of paranasal sinuses is often seen in patients with chronic sinonasal inflammation^(24–26). Although the definition of rhinosinusitis is inflammation of the mucosal lining, evidence reveals that the inflammatory reactions also extend to the underlying bone⁽²⁴⁾. The cytokines and immune signals produced during the inflammation affect the autoregulation of osteoblasts and osteoclasts, and lead to remodelling of the sinus walls, including sclerosis and bony dehiscence of the sinus wall^(25,27). Our results showed that both lateral wall sclerosis and bony dehiscence were more common in patients with SSFB than in patients with USRS. Moreover, lateral wall sclerosis was the most common CT imaging feature. The reason bony remodelling has a stronger association with SSFB than USRS is not fully understood. One possible reason is the insidious and long clinical course before diagnosis in SSFB. Accordingly, SSFB may generally have a longer inflammatory process than that in USRS, which predisposes the bony remodelling of sinus walls in patients with SSFB.

Similar to the reports of previous studies of SSFB demonstrating the predominance of the female sex and older patients^(4,7,16), the mean age was 57.9 ± 14.4 years and the female to male

ratio was 2.7:1 in patients with SSFB in this study. Regarding the strong female predominance of SFB, studies have proposed that hormonal change and a relative small sinus antrum in women may be involved in the pathogenesis of SFB⁽⁴⁾. In addition, given that SFB is more prevalent in older individuals, the longer life expectancy of women may also contribute to this.

Diabetes mellitus was a common comorbidity in patients with SFB^(4,7,16). In this study, there was a high prevalence of diabetes mellitus in patients with SSFB (22.7%) compared to that of 8.4% (2005–2008) and 9.1% (2015–2018) in the general population in Taiwan⁽²⁸⁾. Altered microvascularization of the nasal mucosa with decreased mucociliary clearance and impaired fungal clearance by phagocytes in innate immunity may contribute to this association^(29,30).

One of the notable findings in this study is the potential association between SSFB and lower WBC count compared with USRS, which is rarely mentioned in previous studies. In this study, the mean WBC count in the SSFB group (6623/ μ L) was significantly lower than that in the USRS group (7521/ μ L). In addition, in the univariate regression analysis, lower WBC count was associated with SSFB (OR 0.83). Previous studies have demonstrated that peripheral blood inflammatory cells could reflect the degree of sinus inflammation in chronic rhinosinusitis⁽³¹⁾. Besides, high blood neutrophil-to-lymphocyte and eosinophil-to-lymphocyte ratios are associated with nasal polyp recurrence⁽³²⁾. Although there is no study focusing on WBC count in SFB patients to date, we assumed the milder degree of sinus inflammation in SFB in comparison with mainly bacteria related sinus inflammation in USRS may contribute to this finding. However, we believe that a larger study with more detailed classifications of WBC and SFB is necessary to further explore the association and clarify the potential association between SFB and WBC count.

Due to the lower prevalence of the diagnostic imaging features,

including IH, lateral wall sclerosis, bony dehiscence, and irregular surface, in patients with SSFB compared to those with maxillary SFB, there is a lack of single specific predictor to achieve a precise diagnosis of SSFB before surgery. Therefore, we developed a nomogram model as a novel preoperative diagnostic tool for SSFB according to the aforementioned predictors both in clinical characteristics and CT features. We adopted patients' age, sex, comorbidity of DM, and preoperative WBC counts as diagnostic features in addition to their CT imaging features to further improve the diagnostic accuracy for SSFB. The ROC curve and the calibration curve validated the good discrimination and calibration of this nomogram model. We hope that this nomogram can help clinicians predict the probability of SSFB in patients more accurately to reduce ineffective or delayed treatment and occurrence of complications.

Between CT and MRI for the evaluation of isolated sphenoid sinus diseases, CT is superior in defining the bony structure, and magnetic resonance imaging (MRI) is superior in soft tissue resolution⁽¹⁷⁾. Although abnormal endoscopic findings, such as purulent discharge, mucosal oedema, polyp formation, in the sphenoid recess could be present, normal endoscopic finding can also be present in isolated sphenoid sinus diseases⁽³³⁾. Thus, CT scan is usually done as the first imaging test in the diagnostic workup in patients with specific clinical symptoms. However, an MRI is required when the symptoms are highly suspicious of a sphenoid sinus disease with an intracranial or intraorbital invasion, neoplasm, erosion of the sphenoid sinus wall on CT image or any uncertainty⁽³⁴⁾. In the current study, preoperative MRI was performed for 32 of the total 120 (26.7%) patients with isolated sphenoid sinus diseases. MRI was performed for 9 and 7 patients due to suspected intraorbital or intracranial invasion and suspected presence of tumour, respectively. MRI was performed for the other 16 patients as doctors from other departments requested one during a workup for headache or regular follow-up examinations prior to otolaryngological consultation.

A previous study reported that the sensitivities of CT and MRI in diagnosing inflammatory lesions are 95% and 61%, respectively; while, in tumorous disease, the corresponding values are 72% and 100%, respectively⁽¹⁷⁾. MRI usually demonstrates an iso- or hypointensity and marked hypointensity on T1- and T2-weighted images of SSFB, respectively. However, possible artefacts related to the metal content within fungal hyphae may interfere with the presentation^(11,17,20). The current study focused on comparing the clinical characteristics and CT features between SSFB and USRS and is helpful in differentiating the two most common inflammatory diseases of the sphenoid sinus. Nevertheless, MRI should be used complementarily for evaluating complicated isolated sphenoid sinus diseases to visualize the lesions better and identify intracranial and intraorbital extensions.

There were several limitations in this study. First, only patients

who underwent sinus surgery with a histopathologic diagnosis of SSFB or USRS were recruited in this study. As a result, patients with SSFB and USRS who were ineligible for surgery were not included in this study. This may lead to some degree of selection bias. Second, there were only a few cases with information on fungal species from cultures; however, aspergillus has been reported to be the most common causative organism. Different species of fungi may have different CT imaging features. Future large-scale studies, with larger number of cases may be necessary to investigate the impact of different fungal species on image findings. Finally, this study aimed to distinguish SSFB from non-fungal rhinosinusitis using a retrospective case-control design, and the CT images were specific in identifying SSFB. However, in clinical practice, clinicians may need to consider more differential diagnoses beyond SSFB and USRS, such as neoplasms, mucocele, encephalocele, vascular lesions, etc. Bony erosion or destruction is a common finding on CT scans of these pathologies, and further evaluation with MRI or endoscopic biopsy is necessary for accurate diagnosis⁽³⁴⁾. Thus, a large-scale study with various pathologies in the sphenoid sinus is needed to develop a diagnostic process for a unilateral sphenoid sinus lesion.

Conclusions

We developed a nomogram model as a novel preoperative diagnostic tool for identifying SSFB according to the predictors both in clinical characteristics and on CT features. This could help the clinicians in predicting the probability of SSFB and reduce ineffective or delayed treatment and occurrence of complications.

Acknowledgements

The authors received research grants from the Ministry of Science and Technology (MOST 110-2314-B-182A-100 -) and Chang Gung Memorial Hospital (CMRPG3K2321), Taiwan. The funding agency had no role in the study design, data collection, analysis, decision to publish, or preparation of the manuscript.

Authorship contribution

CCH designed the study. YHF, PWW, YLH, and CCL performed data collection. YHF, PWW, and CCH performed data analysis and drafted the manuscript. PWW, TJL, CCH, and PHC helped with the enrolment of participants and collection of clinical data. PWW and CCH contributed to data interpretation. All authors participated in the scientific discussions and approved the final manuscript.

Conflicts of interest

The authors declare no conflict of interest.

Funding

None.

References

- Chakrabarti A, Denning DW, Ferguson BJ, et al. Fungal rhinosinusitis: a categorization and definitional schema addressing current controversies. *Laryngoscope* 2009;119:1809–1818.
- Wu PW, Huang YL, Yang SW, et al. Acute invasive fungal rhinosinusitis in twenty-one diabetic patients. *Clin Otolaryngol*. 2018;43(4):1163–1167.
- Laury A.M., Wise S.K. Allergic fungal rhinosinusitis. *Am J Rhinol Allergy*. 2013;27(3_suppl):S26–S27.
- Wu PW, Lee TJ, Yang SW, et al. Differences in clinical and imaging presentation of maxillary sinus fungus ball with and without intralesional hyperdensity. *Sci Rep*. 2021;14:11(1):23945.
- Seo MY, Seok H, Lee SH, et al. Microinvasive Fungal Rhinosinusitis: Proposal of a New Subtype in the Classification. *J Clin Med*. 2020; 24;9(2):600.
- deShazo RD, Chapin K, Swain RE. Fungal Sinusitis. *New England Journal of Medicine*. 1997;337(4):254–259.
- Yoon YH, Xu J, Park SK, Heo JH, Kim YM, Rha KS. A retrospective analysis of 538 sinonasal fungus ball cases treated at a single tertiary medical center in Korea (1996–2015). *Int Forum Allergy Rhinol* 2017;7:1070–1075.
- Fadda GL, Allevi F, Rosso C, et al. Treatment of Paranasal Sinus Fungus Ball: A Systematic Review and Meta-Analysis. *Ann Otol Rhinol Laryngol*. 2021;130(11):1302–1310.
- Ledderose GJ, Braun T, Betz CS, Stelter K, Leunig A. Functional endoscopic surgery of paranasal fungus ball: clinical outcome, patient benefit and health-related quality of life. *Eur Arch Otorhinolaryngol* 2012;269: 2203–2208.
- Nicolai P, Lombardi D, Tomenzoli D, et al. Fungus ball of the paranasal sinuses: experience in 160 patients treated with endoscopic surgery. *Laryngoscope*. 2009;119(11):2275–2279.
- Kim TH, Na KJ, Seok JH, Heo SJ, Park JH, Kim JS. A retrospective analysis of 29 isolated sphenoid fungus ball cases from a medical centre in Korea (1999–2012). *Rhinology*. 2013;51(3):280–286.
- Massoubre J, Saroul N, Vokwely JE, Lietin B, Mom T, Gilain L. Results of transnasal transostial sphenoidotomy in 79 cases of chronic sphenoid sinusitis. *Eur Ann Otorhinolaryngol Head Neck Dis*. 2016;133(4):231–236.
- Foanant S, Angkurawaranon S, Angkurawaranon C, Roongrotwattanasiri K, Chaiyasate S. Sphenoid Sinus Diseases: A Review of 1,442 Patients. *Int J Otolaryngol*. 2017;2017:9650910.
- Jung JH, Cho GS, Chung YS, Lee BJ. Clinical characteristics and outcome in patients with isolated sphenoid sinus aspergilloma. *Auris Nasus Larynx*. 2013;40(2):189–193.
- Chen L, Jiang L, Yang B, Subramanian PS. Clinical features of visual disturbances secondary to isolated sphenoid sinus inflammatory diseases. *BMC Ophthalmol*. 2017;17(1):237.
- Ho CF, Lee TJ, Wu PW, et al. Diagnosis of a maxillary sinus fungus ball without intralesional hyperdensity on computed tomography. *Laryngoscope*. 2019;129(5):1041–1045.
- Fawaz SA, Ezzat WF, Salman MI. Sensitivity and specificity of computed tomography and magnetic resonance imaging in the diagnosis of isolated sphenoid sinus diseases. *Laryngoscope*. 2011;121(7):1584–1589.
- Cha H, Song Y, Bae YJ, et al. Clinical Characteristics Other Than Intralesional Hyperdensity May Increase the Preoperative Diagnostic Accuracy of Maxillary Sinus Fungal Ball. *Clin Exp Otorhinolaryngol*. 2020;13(2):157–163.
- Dhong HJ, Jung JY, Park JH. Diagnostic accuracy in sinus fungus balls: CT scan and operative findings. *Am J Rhinol*. 2000;14(4):227–231.
- Eloy P, Grenier J, Pirlet A, Poirrier AL, Stephens JS, Rombaux P. Sphenoid sinus fungall ball: a retrospective study over a 10-year period. *Rhinology*. 2013;51(2):181–188.
- Lim HS, Yoon YH, Xu J, Kim YM, Rha KS. Isolated sphenoid sinus fungus ball: a retrospective study conducted at a tertiary care referral center in Korea. *Eur Arch Otorhinolaryngol*. 2017;274(6):2453–2459.
- Bowman J, Panizza B, Gandhi M. Sphenoid sinus fungal balls. *Ann Otol Rhinol Laryngol*. 2007;116(7):514–519.
- Jiang Z, Zhang K, Huang W, Yuan Q. A preliminary study on sinus fungus ball with microCT and x-ray fluorescence technique. *PLoS One* 2016;11:e0148515.
- Mutijima E, Delvenne P, El-Shazly AE. Osteitis in chronic rhinosinusitis: a histopathological study of human ethmoid bone remodeling in allergic versus non-allergic chronic rhinosinusitis. *Advances in Cellular and Molecular Otolaryngology*. 2014;2(1):23504.
- Nair SP, Meghji S, Wilson M, Reddi K, White P, Henderson B. Bacterially induced bone destruction: mechanisms and misconceptions. *Infect Immun*. 1996;64(7):2371–2380.
- Seo YJ, Kim J, Kim K, Lee JG, Kim CH, Yoon JH. Radiologic characteristics of sinonasal fungus ball: an analysis of 119 cases. *Acta Radiol*. 2011;52(7):790–795.
- Ralston SH, Ho LP, Helfrich MH, Grabowski PS, Johnston PW, Benjamin N. Nitric oxide: a cytokine-induced regulator of bone resorption. *J Bone Miner Res*. 1995;10(7):1040–1049.
- Health Promotion Administration, Ministry of Health and Welfare, Taiwan. Survey on the Prevalence of Hypertension, Hyperglycemia and Hyperlipidemia in Taiwan. Accessed Aug. 3, 2022.
- Chinn RY, Diamond RD. Generation of chemotactic factors by *Rhizopus oryzae* in the presence and absence of serum: relationship to hyphal damage mediated by human neutrophils and effects of hyperglycemia and ketoacidosis. *Infect Immun*. 1982;38(3):1123–1129.
- Müller M, Betlejewski S. Nasal mucosa in patients with diabetes mellitus. *Otolaryngol Pol*. 2003;57(3):361–364.
- Zagólski O, Stręk P, Jurczak W, Gorzedowski P, Zellzahl. Peripheral blood cell count and inflammation-based markers in chronic rhinosinusitis. *HNO*. 2018;66(8):605–612.
- Boztepe OF, Gün T, Demir M, Gür ÖE, Ozel D, Doğru H. A novel predictive marker for the recurrence of nasal polyposis following endoscopic sinus surgery. *Eur Arch Otorhinolaryngol*. 2016;273(6):1439–44.
- Sethi DS. Isolated sphenoid lesions: diagnosis and management. *Otolaryngol Head Neck Surg*. 1999;120(5):730–736.
- Ashida N, Maeda Y, Kitamura T, et al. Isolated sphenoid sinus opacification is often asymptomatic and is not referred for otolaryngology consultation. *Sci Rep*. 2021;7;11(1):11902.

Chien-Chia Huang
 Division of Rhinology
 Department of Otolaryngology
 Chang Gung Memorial Hospital and
 Chang Gung University
 No. 5, Fu-Shin Street
 Kweishan
 Taoyuan 333
 Taiwan

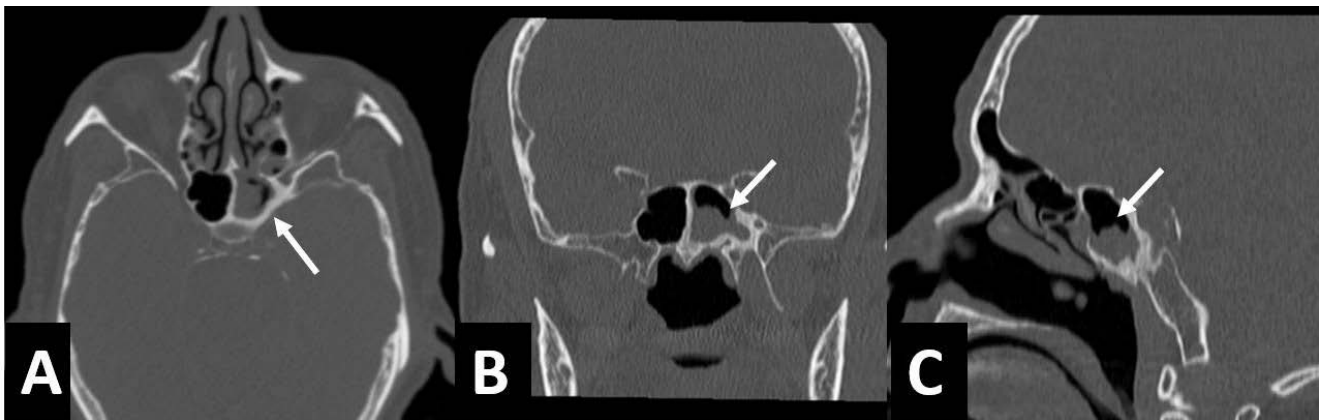
Tel: +886-3-3281200 ext. 8466
 Fax: +886-3-3979361
 E-mail: agar@cgmh.org.tw

SUPPLEMENTARY MATERIAL

Using a nomogram to predict the probability of a sphenoid sinus fungal ball (SSFB) for the patient

Before using the nomogram model, clinicians need to collect the clinical information of the patient as below, which include patient’s age, gender, white blood cell count, and whether the patient has diabetes or not. In addition, the images of sinonasal computed tomography (CT) must be carefully examined from different planes, and the following CT imaging features should be recorded if presented, including the intralesional hyperdensity, bony dehiscence, lateral wall sclerosis, and irregular surface.

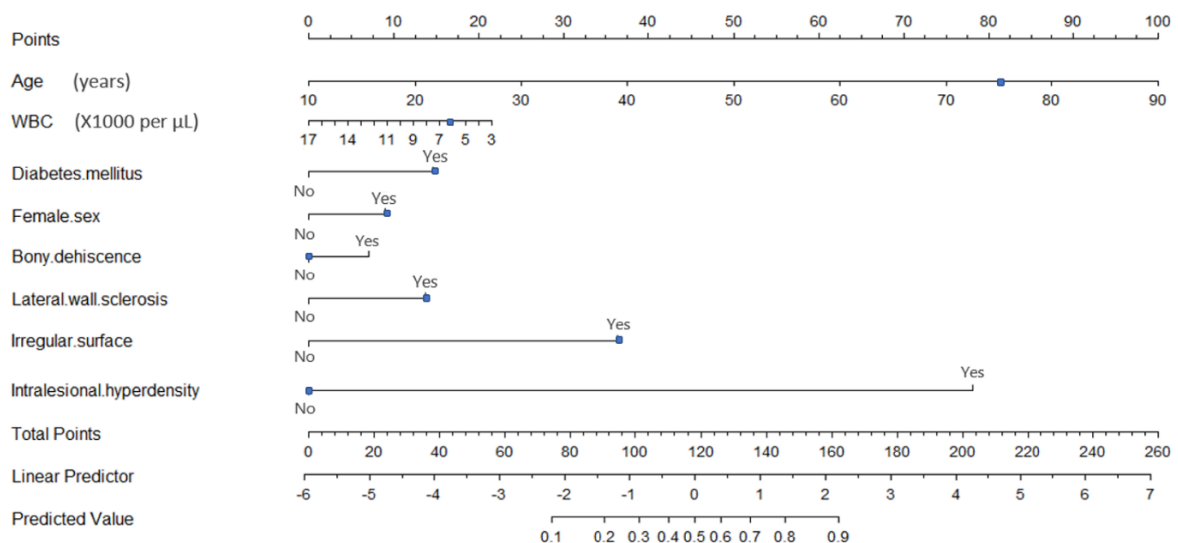
A participant in the study was chosen for displaying the use of the nomogram for the purpose of demonstration. One 75-year-old, diabetic women, presented with post nasal dripping and foul odor smell. Her white blood cell count was 6300 per μL . Upon examining her sinonasal CT images, a partial opacified lesion was noticed in her left sphenoid sinus. There was no intralesional hyperdensity, but lateral wall sclerosis and irregular surface were presented on CT (Supplementary Figure S1). Then, based on the above information, we could use the nomogram to obtain the probability of SSFB for this patient, following the steps in Supplementary Figure S2, which is more than 90%.



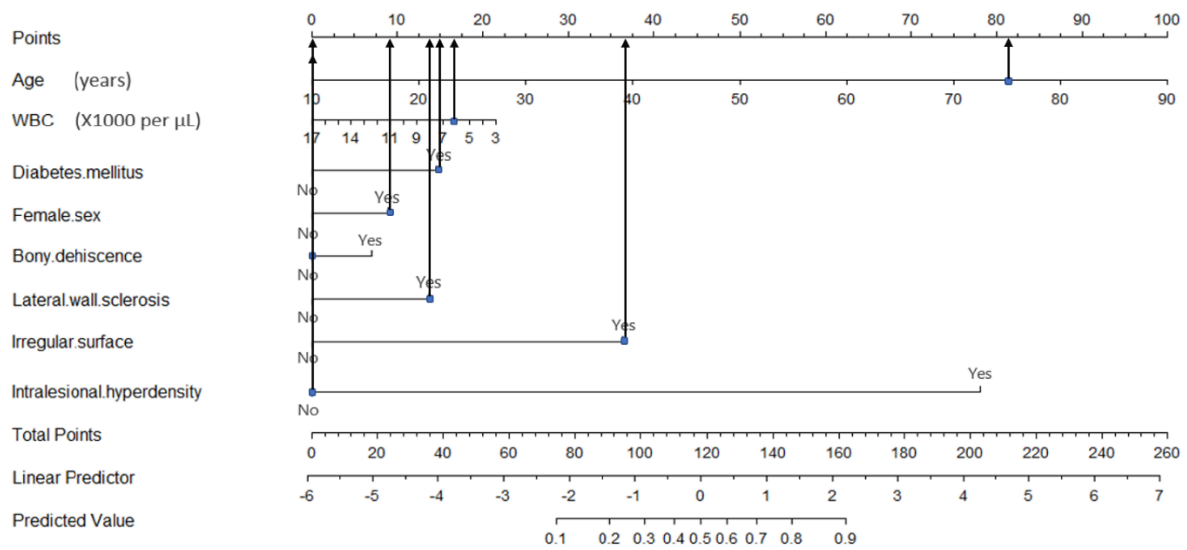
Supplementary Figure 1. Computed tomographic features of patient’s sphenoid sinus lesion. (A) Lateral wall sclerosis. (B) partial opacification, and (C) irregular surface were seen on patient’s computed tomographic images.

Steps for using a nomogram to predict the probability of a sphenoid sinus fungal ball (SSFB).

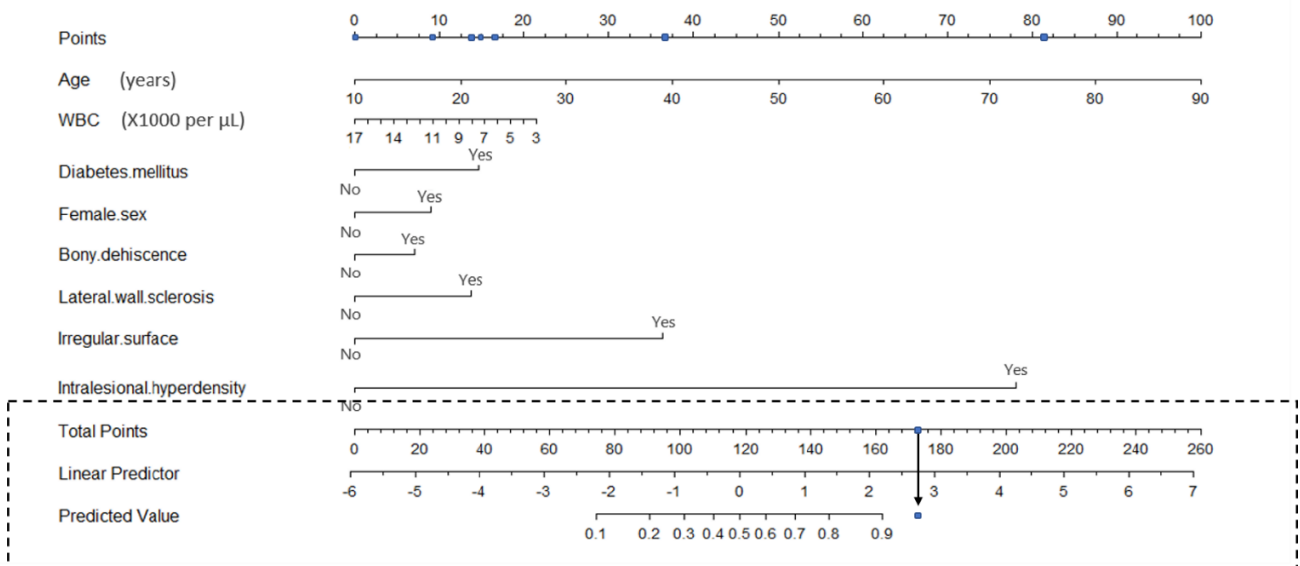
Step 1. Find the corresponding position of each variable according to the patient’s clinical information and radiological characteristics.



Step 2. Next, draw a line vertically upward to the Points axis above to obtain the respective points for each variable. After that, calculate the total points by adding up the respective points for each variable. For this patient, her total points are 173 points.



Step 3. Finally, drew a line vertically downward from the corresponding position on the Total Points axis to the Predicted Value axis to obtain the probability of SSFB. For this patient, the probability of SSFB is more than 90%.



Abbreviation: WBC, white blood cell count.